by determining spectrometrically the extent of ionization for *p*-anisyldiphenylmethanol and correlated it with the known pK_{R^+} value (-1.24)[37] of *p*-anisyldiphenylmethyl cation.

The pK_{R^+} values for the monocations and also the values corresponding to the second neutralization of the dications were determined at 25 °C in 50% acetonitrile by means of the UV spectrophotometric method described in a previous paper.[38]

Cyclic Voltammetry. The measurements were done with the method and apparatus described in the previous paper.[38] Sample solutions were 1 mM in cation and 0.1 M in tetrabutylammonium perchlorate as a supporting electrolyte. Scan rate was 0.1 V/s. All the cations exhibited the irreversible cathodic peak at the potential given in Table V. Immediately after each measurement, ferrocene (0.2 mM) was added as an internal standard,[39] and the peak potential was corrected with reference to this standard.

Acknowledgment. We thank Shigeo Fujii of Tottori University for technical assistance in the X-ray crystallographic analysis. Helpful discussion with Professor Hiroshi Fujimoto of Division of Molecular Engineering, Faculty of Engineering, Kyoto University, is gratefully acknowledged.

Supplementary Material Available: Tables of all the bond lengths and angles, of atomic coordinates and thermal parameters, and of anisotropic thermal parameters and a table of melting points and spectral data for the tetrafluoroborates of cations **3**, **24**, **26**, and **28** (7 pages). Ordering information is given on any current masthead page.

(38) Komatsu, K.; Masumoto, K.; Waki, Y.; Okamoto, K. *Bull. Chem. Soc. Jpn.* **1982**, *55*, 2470.

(39) Gagne, R. R.; Koval, C. A.; Lisensky, G. C. *Inorg. Chem.* **1980**, *19*, 2854.

Perpendicular Effects on Transition States. 2. Energy Profiles and Reaction Surfaces

Noam Agmon

Department of Physical Chemistry, The Hebrew University, Jerusalem 91904, Israel

Received October 27, 1986

It is shown how the free energy profiles along and perpendicular to the reaction coordinate determine a two-dimensional energy surface for describing substituent effects in organic reactivity. This affords a generalization of the hyperbolic–paraboloid surfaces, extendible to large energy variations. It also shows that the reaction surface and curve-crossing approaches lead to a similar mathematical description of the problem. The various models are compared with experimental results for free energy of activation of proton-transfer reactions between benzoic acids and methanol and of Cope and Claisen rearrangements.

Use of two-dimensional plots to discuss effects along and perpendicular to the reaction coordinate has become increasingly popular.[1-16] In this picture, substituents can affect the free energy of activation (that is, the energy of the saddle point in the two-dimensional free energy surface) in two ways: The free energies of reactants and products (G_1, G_2) along the reaction coordinate may vary, resulting in the customary Hammond effect,[17,18] or the free energies of the perpendicular structures (G_3, G_4) may be perturbed, leading to an anti-Hammond effect,[3] where the transition state moves *toward* the state of lowered energy.

Most authors who model such surfaces quantitatively[6,12,14,16] use a hyperbolic–paraboloid function, namely a quadratic polynomial in two variables, with parameters determined so that the surface has a maximum along one direction and a minimum along the perpendicular direction. Such a potential necessarily reduces[14] to Marcus'[19] quadratic energy profile along the reaction coordinate. This is rather restrictive, especially since the Marcus relation is not expected to give a good description of experiment over a large energy range.[20]

Since much more is known on the general form of the profile along the reaction coordinate[20] than on the shape of the surface, it seems natural to begin its construction from such profiles. This has been my approach in a recent publication.[15] That model (model I) is based on a free

(1) Hughes, E. D.; Ingold, C. K.; Shapiro, U. G. *J. Chem. Soc.* **1936**, 225-236.
(2) Thornton, E. R. *J. Am. Chem. Soc.* **1967**, *89*, 2915-2927.
(3) More O'Ferrall, R. A. *J. Chem. Soc. B* **1970**, 274-277.
(4) Harris, J. C.; Kurz, J. L. *J. Am. Chem. Soc.* **1970**, *92*, 349-355.
(5) Critchlow, J. E. *J. Chem. Soc., Faraday Trans. 1* **1972**, *68*, 1774-1792.
(6) (a) Jencks, W. P. *Chem. Rev.* **1972**, *72*, 705-718. (b) Jencks, D. A.; Jencks, W. P. *J. Am. Chem. Soc.* **1977**, *99*, 7948-7960. (c) Funderback, L. H.; Aldwin, L.; Jencks, W. P. *J. Am. Chem. Soc.* **1978**, *100*, 5444-5459. (d) Jencks, W. P. *Chem. Rev.* **1985**, *85*, 511-527.
(7) Dunn, B. M. *Int. J. Chem. Kinet.* **1974**, *6*, 143-159.
(8) Bruice, T. C. *Annu. Rev. Biochem.* **1976**, *45*, 331-373.
(9) Wehrli, R.; Schmid, H.; Belluš, D.; Hansen, H.-J. *Helv. Chim. Acta* **1977**, *60*, 1325-1356.
(10) (a) Albery, J.; Kreevoy, M. M. *Adv. Phys. Org. Chem.* **1978**, *16*, 87-157. (b) Kreevoy, M. M.; Lee, I.-S. H. *J. Am. Chem. Soc.* **1984**, *106*, 2550-2553.
(11) Harris, J. M.; Shafer, S. G.; Moffatt, J. R.; Becker, A. R. *J. Am. Chem. Soc.* **1979**, *101*, 3295-3299.
(12) (a) Gajewski, J. J. *J. Am. Chem. Soc.* **1979**, *101*, 4393-4394. (b) Gajewski, J. J.; Gilbert, K. E. *J. Org. Chem.* **1984**, *49*, 11-17.
(13) Buncel, E.; Wilson, H.; Chuaqui, C. *J. Am. Chem. Soc.* **1982**, *104*, 4896-4900.
(14) Murdoch, J. R. *J. Am. Chem. Soc.* **1983**, *105*, 2660-2667.
(15) Agmon, N. *J. Am. Chem. Soc.* **1984**, *106*, 6960-6962.
(16) (a) Grunwald, E. *J. Am. Chem. Soc.* **1985**, *107*, 125-133. (b) Grunwald, E. *J. Am. Chem. Soc.* **1985**, *107*, 4710-4715.

(17) Hammond, G. S. *J. Am. Chem. Soc.* **1955**, *77*, 334-338.
(18) Agmon, N. *J. Chem. Soc., Faraday Trans. 2* **1978**, *74*, 388-404.
(19) Marcus, R. A. *J. Phys. Chem.* **1968**, *72*, 891-899.
(20) Agmon, N. *Int. J. Chem. Kinet.* **1981**, *13*, 333-365 and references therein.

0022-3263/87/1952-2192$01.50/0

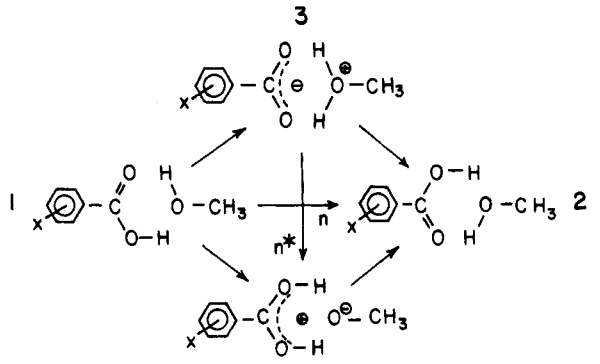

Figure 1. Identity proton-transfer reactions between substituted benzoic acids and methanol. Reaction proceeds from structure 1 to structure 2 with structures 3 and 4 as possible intermediates. The concerted path is the reaction coordinate n. The perpendicular coordinate (the disparity mode[16a]) is n^*.

energy profile along the reaction coordinate and an upside-down profile along the perpendicular coordinate. With a few simple assumptions it was possible[15] to describe both Hammond and anti-Hammond effects, in agreement with experimental data.

The energy profile model (model I) does not require specification of the complete reaction surface. Hence, it can also be interpreted as arising from the avoided crossing of two configurations in the valence-bond approach,[21] in reactions where the electronic configurations of 1 and 4, and also those of 2 and 3, are the same. Still another interpretation is that of an excited electronic curve, G_3G_4, and a ground-state potential, G_1G_2, which are mutually dependent. The purpose of the present discussion is to show how two such profiles explicitly determine a reaction surface (model II) whose sections along two perpendicular directions coincide with the given profiles. Numerically the difference between the two models is small, which shows that the curve-crossing and reaction-surface pictures lead to a similar mathematical description.

The hyperbolic–paraboloid surface found in the literature is a special case of model II, for parabolic energy profiles. Use of profiles that were shown[20] to apply for a large energy range produces surfaces with a larger range of applicability. This is the practical merit of the method. Unfortunately, experimental data at present do not cover a large enough free energy range to test this conclusion, as shown by a comparison of the different models with the free energy of activation for three families of reactions: identity proton-transfer reactions and Cope and Claisen rearrangements.

Energy Profiles

Here previous results concerning free energy profiles are reviewed. Consider as an example the identity proton-transfer reactions between substituted benzoic acids and methanol (Figure 1). The reactants and products (structures 1 and 2) are here identical. Their concerted interconversion is described by the reaction-coordinate variable n, which assumes values between 0 (for reactants) and 1 (for products). The two perpendicular structures, 3 and 4, are the bond-breaking and bond-making configurations. Their interconversion defines the perpendicular coordinate, n^*, which by assumption also varies between 0 and 1.

(21) (a) Pross, A.; Shaik, S. S. *Acc. Chem. Res.* **1983**, *16*, 363–370. (b) Pross, A. *Adv. Phys. Org. Chem.* **1985**, *21*, 99–196.

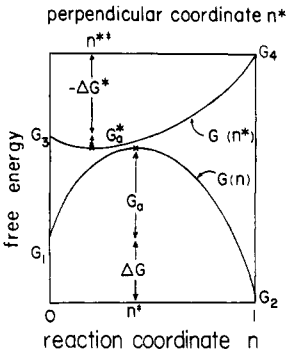

Figure 2. Free energy profiles (model I): The bottom reaction profile is $G_1 + G(n,\Delta G;G_a^0)$, while the upper inverted profile is $G_3 - G(n^*,\Delta G^*;G_a^0)$. The function G is given by eq 3 and 6. The designation of the four structures corresponds to that of Figure 1. Theie energies are the same as in Figure 1 of ref 15.

In terms of bond orders, it is n^* that measures the total bond order in the benzoic acid. A constant n^* implies bond-order conservation such as along the concerted pathway defined by the coordinate n. The configuration of the transition state is given by some value of these coordinates, denoted by $n^‡$ and $n^{*‡}$. The transition state may be called early or late, depending on whether $n^‡$ is smaller or larger than $^1/_2$, respectively. It is loose or tight when $n^{*‡}$ is smaller or larger than $^1/_2$, respectively.

In model I all that matters is the shape of the two energy profiles, as a function of n and n^*. The lower profile is the usual free energy profile along the reaction coordinate, while the upper profile is an inverted one. This is demonstrated in Figure 2.

In order that the model be usable three simple assumptions are made:

(i) The two profiles have the same functional dependence $G(x,\Delta;\Gamma)$ on the independent coordinate x, the free energy gap between the two end points Δ, and a parameter Γ. If $G(0,\Delta;\Gamma) = 0$ and $G(1,\Delta;\Gamma) = \Delta$, then the lower profile is given by $G_1 + G(n,\Delta G;G_a^0)$ while the upper one is $G_3 - G(n^*,\Delta G^*;G_a^{0*})$. $\Delta G \equiv G_2 - G_1$ while $\Delta G^* \equiv G_3 - G_4$. G_a^0 and G_a^{0*} will be called intrinsic barriers.[19] Finally, the barrier height in the lower profile will be denoted by $G_a \equiv G(n^‡,\Delta G;G_a^0)$, while the well depth in the upper profile is $G_a^* \equiv G(n^{*‡},\Delta G^*;G_a^{0*})$.

(ii) The minimum in the upper profile coincides in energy with the maximum in the lower profile:

$$G_a + G_a^* = G_3 - G_1 \tag{1}$$

This is the energy of the crossing point in the curve-crossing picture, or the energy of the saddle point in the reaction surface model. $n^‡$ and $n^{*‡}$ are of coarse not identical, since n and n^* are independent variables.

(iii) The two intrinsic barriers are proportional to each other:

$$G_a^{0*} = rG_a^0 \tag{2}$$

This is better than taking one of the intrinsic barriers constant, which cannot be true in the limit that all energy spacings decrease to zero.

One notes that three parameters have been defined: G_a^0, G_a^{0*}, and r. There are two equations connecting these parameters, eq 1 and 2. Hence the model has only one free parameter to be determined from a fit to experiment.

To apply the model, one needs an explicit expression for the free energy profile along the reaction coordinate, $G(x,\Delta;\Gamma)$. This is given by the general expression[20]

$$G(x,\Delta;\Gamma) = x\Delta + \Gamma M(x) \tag{3}$$

where $M(x)$ is a mixing function. Let us mention two such

functions. The first is an inverted parabola:

$$M(x) = 4x(1 - x) \quad (4)$$

It leads to the linear dependence of the transition-state location and the parabolic dependence of its free energy on Δ, which are the Marcus theory results:[19]

$$x^{\ddagger}(\Delta;\Gamma) = (1 + \Delta/4\Gamma)/2 \quad (5a)$$

$$G(x^{\ddagger},\Delta;\Gamma) = \Gamma(1 + \Delta/4\Gamma)^2 \quad (5b)$$

Another mixing function is the entropy function

$$M(x) = -[x \ln x + (1 - x) \ln (1 - x)]/\ln 2 \quad (6)$$

which gives

$$x^{\ddagger}(\Delta;\Gamma) = [1 + \exp(-\Delta \ln 2/\Gamma)]^{-1} \quad (7a)$$

$$G(x^{\ddagger},\Delta;\Gamma) = -\Gamma \ln (1 - x^{\ddagger})/\ln 2 \quad (7b)$$

Over a limited range in Δ the difference between eq 5 and 7 is small but becomes appreciable for a large energy range ($|\Delta| > 4\Gamma$). Under these conditions, eq 5b shows an inverted behavior, which is not relevant to atom- (or group-) transfer reactions. We therefore use eq 6 in model I, but notice that any desired expression for the energy profile along the reaction coordinate could be inserted into our equations.

Reaction Surfaces

Now a two-dimensional free energy surface, $g(n,n^*)$, is constructed so that sections along and perpendicular to the reaction coordinate coincide with the two above-mentioned profiles:

$$g(n,{}^1/_2) = G_1 + G(n,\Delta G;G_a^0) \quad (8a)$$

$$g({}^1/_2,n^*) = G_3 - G(n^*,\Delta G^*;G_a^{0*}) \quad (8b)$$

This can be easily achieved by superimposing the two profiles

$$g(n,n^*) = G(n,\Delta G;G_a^0) + G_3 - G(n^*,\Delta G^*;G_a^{0*}) - G({}^1/_2,\Delta G;G_a^0) \quad (9)$$

which already fulfills eq 8b. To account for eq 8a we demand that

$$G_3 - G_1 = G({}^1/_2,\Delta G;G_a^0) + G({}^1/_2,\Delta G^*;G_a^{0*}) \quad (10)$$

This relates the two intrinsic barriers. Note that for all reaction profiles given by the general relation (3), for whith $M({}^1/_2) = 1$, one has

$$G({}^1/_2,\Delta;\Gamma) = \Gamma + {}^1/_2\Delta \quad (11)$$

Hence eq 10 reads

$$G_a^0 + G_a^{0*} = (G_4 + G_3 - G_2 - G_1)/2 \quad (10')$$

This coincides with eq 6 of ref 16a, which (see below) is a special case of the present formalism.

A free energy surface, $g(n,n^*)$, is shown in Figure 3, for n and n^* in the range 0–1. It corresponds to the profiles of in Figure 2. The four structures (e.g., Figure 1) are at $(0,{}^1/_2)$, $(1,{}^1/_2)$, $({}^1/_2,0)$, and $({}^1/_2,1)$, respectively. Usually, only the area inside the smaller square is of interest.

It is now shown how the two conditions in eq 1 and 2 are obeyed. For $\Delta G = \Delta G^* = 0$, eq 10′ reduces to

$$G_a^0 + G_a^{0*} = G_3 - G_1 \quad (10'')$$

This is a special case of eq 1. In the more general situation, eq 1 is obeyed only approximately: The two coordinates in model I are better interpreted as curvilinear coordinates through the saddle point in Figure 3, instead of the straight lines of model II. This is the reason for numerical differences between the two models.

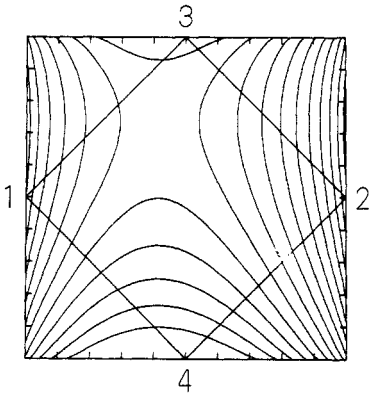

Figure 3. Reaction free energy surface (model II) derived from the two profiles of Figure 2 using eq 9. The four structures are the corners of the inner square, corresponding to the situation in Figure 1. Equipotentials shown are from −20 (structure 2) to +60 (at structure 4) kcal/mol, every 5 kcal/mol. n is the x axis, while n^* is the $-y$ axis. The saddle point is located at $n^{\ddagger} = 0.42$ and $n^{*\ddagger} = 0.20$.

Equation 2 is easily introduced into the condition (10′) to give

$$G_a^0 = (G_4 + G_3 - G_2 - G_1)/2(1 + r) \quad (12)$$

This establishes the free energy of activation, $g(n^{\ddagger},n^{*\ddagger}) - G_1$, as an explicit function of the free energies of the four corners and the single parameter r.

As in model I, different functional forms for the free energy along the reaction coordinate lead to different functional forms for the reaction surface. A quadratic profile, eq 4, when inserted into eq 9 gives

$$g(n,n^*) = n\Delta G + 4G_a^0 n(1 - n) - n^*\Delta G^* - 4G_a^{0*}n^*(1 - n^*) + G_3 - G_a^0 - {}^1/_2\Delta G \quad (13)$$

which coincides with the hyperbolic–paraboloid surfaces of the literature.[14,16] In the framework of the more general model outlined here, eq 6 is chosen as the basis for the free energy profile along the reaction coordinate, because of its applicability to a larger ΔG range. This yields

$$G_a \equiv g(n^{\ddagger},n^{*\ddagger}) - G_1 = G_a^0[r \ln(1 - n^{*\ddagger}) - \ln (1 - n^{\ddagger})]/\ln 2 + G_3 - G_1 - G_a^0 - {}^1/_2\Delta G \quad (14)$$

where, due to the fact that n and n^* are uncoupled in eq 9, $n^{\ddagger}(\Delta G;G_a^0)$ and $n^{*\ddagger}(\Delta G^*;G_a^{0*})$ are given by the same relation (7a) as before. G_a^0 and r are related by eq 12.

Results

The results are compared (Tables I–III) of the two models discussed above, the hyperbolic–paraboloid model (eq 13) used in the literature, and recently compiled experimental data for the free energy of activation, G_a, for three reaction series: (i) proton exchange between substituted benzoic acids and methanol (in methanol at 25 °C) [data for these identity ($\Delta G = 0$) reactions obtained by dynamical NMR methods];[16a] (ii) Cope rearrangement of substituted hexadienes; (iii) Claisen rearrangement of allyl vinyl ethers. Data for (ii) and (iii) are from the compilation of ref 12b.

The tables show the input data for the calculation, which are ΔG,ΔG^*, and $G_3 - G_1$. The free energy of activation, G_a, for the different models is given together with the mean square root deviation (msd), mean absolute deviation (mad), and maximal deviation (maxd) of calculation from experiment. Some additional output from the calculation with model I is also shown (there is only a small difference

Table I. Proton Exchange of Benzoic Acids in Methanol (See Figure 1; for These Identity Reactions $\Delta G = 0$ and $n^* = {}^1/_2$; All Energies in kcal/mol)

	input data		barrier height, G_a					minimum location, n^*	
X	ΔG^*	G_3	*a*	*b*	*c*	*d*	*e*	*b*	*d*
H	19.08	12.83	10.88	10.88	11.12	10.97	11.27	0.22	0.15
m-NO_2	21.49	11.37	10.28	10.17	10.15	10.16	10.16	0.19	0.11
p-NO_2	21.64	11.36	10.15	10.14	10.19	10.16	10.15	0.19	0.11
3,5-$(NO_2)_2$	23.90	9.93	9.40	9.38	9.13	9.23	8.99	0.15	0.07
o-NO_2	23.10	10.31	9.30	9.65	9.38	9.47	9.30	0.16	0.08

[a] Experimental.[16a] [b] Grunwald's calculation,[16a] using both intrinsic barriers as free parameters (i.e., ignoring eq 10'); msd = 0.16, mad = 0.10, maxd = 0.35 kcal/mol. [c] Hyperbolic–paraboloid model, eq 13, with $G_a^{0*} = 8.6$ kcal/mol and G_a^0 evaluated from eq 10'; msd = 0.18, mad = 0.15, maxd = 0.27 kcal/mol. [d] Model I with $r = 0.706$; msd = 0.12, mad = 0.11, maxd = 0.17 kcal/mol. [e] Model II with $r = 0.478$; msd = 0.26, mad = 0.19, maxd = 0.41 kcal/mol.

Table II. Cope Rearrangement of Hexadiene Derivatives (All Energies in kcal/mol)

	input data[12b]				barrier heights, G_a						
reactant	ΔG	ΔG^*	G_3	G_a^{0c}	*a*	*b*	*c*	*d*	G_a^{*c}	n^{*c}	n^{*c}
1,5-hexadiene (chair)	0	4	57	41.6	41	40.9	41.6	41.8	15.4	0.50	0.55
2-phenyl-1,5-hexadiene (chair)	0	14	57	36.8	35.5	37.4	36.8	36.7	20.2	0.50	0.70
3-phenyl-1,5-hexadiene (chair)	−5	−6	47	39.5	37.5	37.1	37.1	37.3	9.9	0.48	0.42
2,5-diphenyl-1,5-hexadiene (chair)	0	24	57	30.6	31	32.0	30.6	30.0	26.4	0.50	0.85
2,5-dicyano-3-methyl-1,5-hexadiene (chair)	−3	21	54	31.4	31	31.5	29.9	29.5	24.1	0.48	0.81
threo-3,4-dimethyl-1,5-hexadiene (chair)	−5	0	53	42.0	39	38.8	39.6	39.8	13.4	0.48	0.50
threo-3,4-diphenyl-1,5-hexadiene (chair)	−10	−16	37	36.3	31	32.3	31.5	31.5	5.5	0.45	0.28
2,4-diphenyl-1,5-hexadiene (chair)	−5	4	47	35.8	34	34.7	33.4	33.6	13.6	0.48	0.56
allyl phenyl ether	5	−22	47	39.6	42	41.7	42.2	41.8	4.8	0.52	0.23
allyl acetate	0	−15	52	44.1	45	42.4	44.1	44.0	8.0	0.50	0.32

[a] Experimental data from Table I of ref 12b. [b] From eq 8 of ref 12b with $a = -27$ kcal/mol. There is probably a printing error for entry 8 in Table I there. msd = 1.19, mad = 0.90, maxd = 2.6 kcal/mol. [c] Model I with $r = 0.32$; msd = 0.73, mad = 0.66, maxd = 1.3 kcal/mol. [d] Model II with $r = 0.312$; msd = 0.87, mad = 0.76, maxd = 1.5 kcal/mol.

Table III. Claisen Rearrangements of Allyl Vinyl Ethers (All Energies in kcal/mol)

	input data				barrier heights, G_a						
reactant	ΔG	ΔG^*	G_3	G_a^{0c}	*a*	*b*	*c*	*d*	G_a^{*c}	n^{*c}	n^{*c}
allyl vinyl ether	−17	−10	47	42.2	33.6	33.6	34.3	34.4	12.7	0.43	0.40
1-cyano allyl vinyl ether	−13.5	−19	41.5	39.4	33.1	32.8	33.1	32.7	8.4	0.44	0.31
2-cyano allyl vinyl ether	−17	−0.5	47	39.2	29.7	31.6	31.3	31.6	15.7	0.43	0.49
4-cyano allyl vinyl ether	−20.5	−19	38	39.0	29.8	29.7	29.7	29.7	8.3	0.41	0.30
5-cyano allyl vinyl ether	−17	−0.5	47	39.2	31.8	31.6	31.3	31.6	15.7	0.43	0.49
6-cyano allyl vinyl ether	−13.5	−19	41.5	39.4	34.6	32.8	33.1	32.7	8.4	0.44	0.31

[a] Experimental data from Table IV of ref 12b. [b] From eq 8 of ref 12b with $a = 23.5$ kcal/mol. This is a better fit than that presented in ref 12b. msd = 1.06, mad = 0.72, maxd = 1.9 kcal/mol. [c] Model I with $r = 0.407$; msd = 0.98, mad = 0.73, maxd = 1.6 kcal/mol. [d] Model II with $r = 0.415$; msd = 1.16, mad = 0.90, maxd = 1.9 kcal/mol.

in transition-state location between the two models). Agreement with experiment in all cases is good. Model I tends to give slightly better results, but more extensive data over a wider energy range would be needed before definite conclusions could be made.

Conclusion

In was shown how a reaction surface depicting substituent effects along and perpendicular to the reaction coordinate can be constructed once the functional form for the energy along the reaction coordinate is given. The hyperbolic–paraboloid surface found in the literature is a special case obtained for a parabolic reaction profile. Improved energy profiles may lead to reaction surfaces valid over much wider energy ranges. Another way in which the present approach differs from others is in the choice of the free parameter, taken here as the ratio of the two intrinsic barriers.

The above exposition shows that the Hammond/anti-Hammond behavior is determined quantitatively from the shape of the profiles along and perpendicular to the reaction coordinate. The concept of a reaction surface is an important guide to our intuition but is not a necessary ingredient in the model. The two profiles may be interpreted as sections through this surface, as well as in other ways. For example, they may originate from the avoided crossing of two different configuration curves, suggesting that the perpendicular structures actually belong to an excited, rather than the ground, electronic state. In empirical models it is difficult to distinguish between different physical descriptions, leading to a similar mathematical formulation.

Acknowledgment. I thank Profs. E. Grunwald and W. P. Jencks for correspondence.

Registry No. MeOH, 67-56-1.